

## Anomalous Plasticity in the Cyclic Torsion of Micron Scale Metallic Wires

Dabiao Liu,<sup>1,2</sup> Yuming He,<sup>1,2,\*</sup> D.J. Dunstan,<sup>3</sup> Bo Zhang,<sup>1,2</sup> Zhipeng Gan,<sup>1,2</sup> Peng Hu,<sup>1,2</sup> and Huaming Ding<sup>1,2</sup>

<sup>1</sup>*Department of Mechanics, Huazhong University of Science and Technology, Wuhan 430074, China*

<sup>2</sup>*Hubei Key Laboratory of Engineering Structural Analysis and Safety Assessment, Wuhan 430074, China*

<sup>3</sup>*School of Physics and Astronomy, Queen Mary University of London, London E1 4NS, United Kingdom*

(Received 21 December 2012; revised manuscript received 29 April 2013; published 11 June 2013)

The plasticity of micron scale Cu and Au wires under cyclic torsion is investigated for the first time by using a torsion balance technique. In addition to a size effect, a distinct Bauschinger effect and an anomalous plastic recovery, wherein reverse plasticity even occurs upon unloading, are unambiguously revealed. The Bauschinger effect and plastic recovery have been observed in molecular dynamics and discrete dislocation dynamics simulations of ideal single-crystal wires; the results here are an excellent confirmation that these effects also occur in experiment in nonideal polycrystalline wires. A physical model consistent with the simulations is described in which the geometrically necessary dislocations induced by the nonuniform deformation in torsion play the key role in these anomalous plastic behaviors.

DOI: [10.1103/PhysRevLett.110.244301](https://doi.org/10.1103/PhysRevLett.110.244301)

PACS numbers: 46.35.+z, 61.72.Hh, 62.20.fq, 62.20.me

The plasticity of small-volume metals has been attracting tremendous attention. A size effect manifested as “smaller is stronger” has been observed in various geometries and different loading conditions, such as wire torsion [1–4], foil bending [5], micro- and nanoindentation [6], and uniaxial tests on micro- and nanopillars [7–11], etc. Until now, much research has focused on the monotonic loading conditions; only a few attempts [12–18] have been devoted to studying cyclic plasticity at small scales. Recently, an interesting recoverable plasticity was experimentally observed in freestanding nanocrystalline films [19] and in an Au nanocrystal under off-axial tensile loading [20] and then confirmed by simulations [21–23]. A similar phenomenon has also been found in other kinds of micromechanics tests [12–14,16]. In practice, the failure of small-scale structures in service is usually due to cyclic loading [24]. Therefore, it is instructive to study cyclic plasticity under inhomogeneous deformation, which enables the analysis of size effects, strain hardening, the Bauschinger effect (BE), and plastic recovery [also known as the anomalous BE].

Several anomalous plastic properties have been predicted in molecular dynamics (MD) and discrete dislocation dynamics (DDD) simulations of thin metal wires under cyclic torsion [17,25,26]. We report cyclic torsion tests on micron scale Cu and Au wires. The size effect, a significant BE, and a plastic recovery are clearly observed, giving direct experimental evidence for the phenomena seen in simulations.

Thin metal wires are studied by using a torsion balance [4], as illustrated in Fig. 1(a). Briefly, it permits the measurement of torque to nN m, as a function of torsional strain to a sensitivity of 0.1 microstrain. Both twist-control and torque-control modes are provided. Twist control is used for cyclic and monotonic strain hardening, the size effect, and the BE. Torque control is used for creep and plastic recovery upon repeated loading.

Tests were conducted on numerous wires of polycrystalline Cu (99.999% purity) with diameter  $2a = 18, 20, 35,$  and  $42 \mu\text{m}$  and polycrystalline Au (99.99% purity) with  $2a = 20 \mu\text{m}$ . The shear strain rate at the surface of the wire was below  $10^{-3}/\text{s}$ . All the Cu wires were annealed at  $410^\circ$  for 2.4 h in a vacuum furnace, while the Au wires were used as supplied (annealed for a few minutes at  $500^\circ\text{C}$ ). The grain size of the Cu wires was measured to be from 5 to  $9 \mu\text{m}$  [see Figs. S1(a) and S1(b) in the Supplemental Material [27]]. Therefore, the Hall-Petch effect here is similar in the different size wires. The average grain size of the Au wire is much smaller, around  $0.87 \pm 0.05 \mu\text{m}$  [see Fig. S1(c) in Ref. [27]]. The texture has not been controlled, but we assume that the annealing has normalized the microstructure and reduced the effect of any preferred orientation.

A typical experimental curve for Cu wire with  $2a = 20 \mu\text{m}$  is shown in Fig. 1(b). The normalized torque  $Q/a^3$  is plotted against the surface shear strain  $\kappa a$ , where  $\kappa$  is the twist per unit length. This specimen was twisted to 1% strain forward and reverse ten times. The initial departure from the origin follows the theoretical elastic response to 75 MPa, and then plasticity is observed. The stress continues to rise to 140 MPa at the strain of 1%, and we refer to this as monotonic hardening. A further increase in normalized torque is seen on each successive cycle, referred to as cyclic hardening. The most dramatic feature in the cyclic response is the plastic recovery  $\varepsilon_{\text{rp}}$ , which initiates even before the torque is reversed.

Typical results for other diameters and with different strain amplitudes are shown in Fig. 2. For each diameter, the specimen was loaded to a prescribed strain, then unloaded, and reverse loaded one or more times to the same strain. Then, it was unloaded entirely. This sequence was repeated to successively larger prescribed strains. Figures 2(a)–2(c) show the responses to three, seven, and

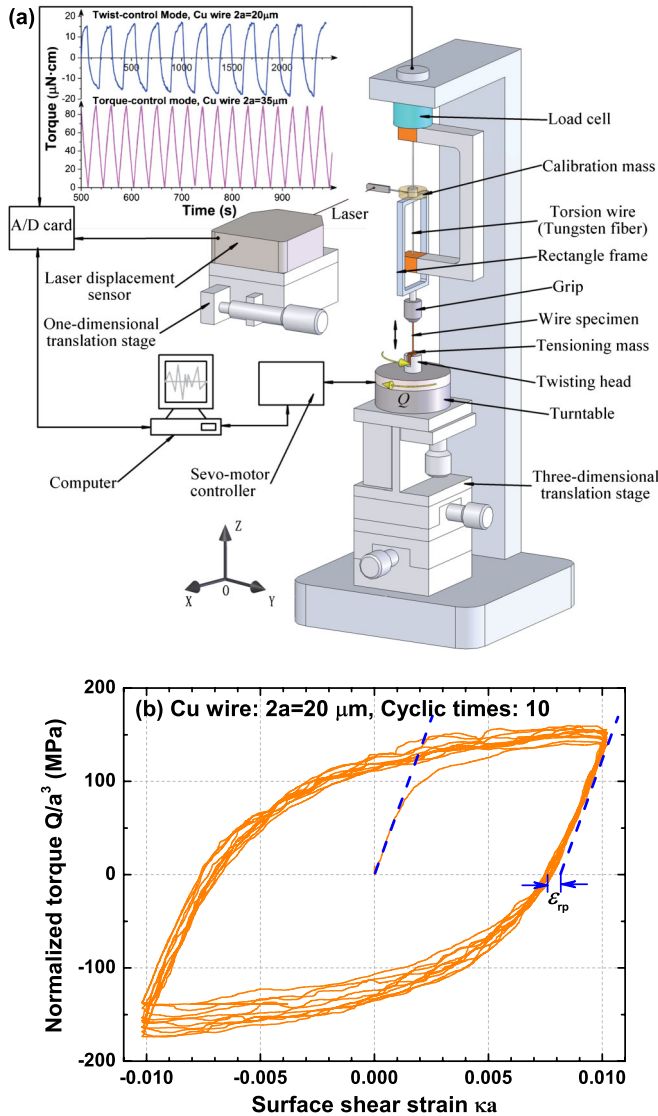


FIG. 1 (color online). (a) Schematic of the experimental apparatus. Typical time dependence of torque in two modes is shown in the inset. (b) Typical cyclic torsion data for a Cu wire with  $2a = 20 \mu\text{m}$  under twist control. The broken straight lines show the elastic response. The plastic strain recovery upon unloading  $\epsilon_{rp}$  is marked on the plot.

six successively greater strains for the Cu wires with  $2a = 18, 35,$  and  $42 \mu\text{m}$ , respectively. Both monotonic and cyclic hardening are seen. For a small strain amplitude ( $\leq 0.005$ ), the Cu wires seem to be cyclically stable [see the first loading in Figs. 2(b) and 2(c)], perhaps because the plasticity has not yet initiated completely at such small strain. At higher strains, above  $\sim 0.005$ , the cyclic hardening becomes evident and then gradually saturates after around ten loops [see the second loading in Figs. 2(b) and 2(c)]. The reverse hardening rates are always higher than that in forward loading [Figs. 1(b) and 2(a)–2(c)]. A strong BE is manifested by (i) the yield strength in the reverse direction is much lower than in the forward

loading, often the plastic deformation starts even during unloading, and (ii) all curves show a smooth transition in the elastic-plastic regime of the reverse loading. Figure 2(d) shows the data for the Au wire. They display an elastic-perfect plasticity, in which neither cyclic hardening nor monotonic hardening are observed; however, a pronounced BE does occur.

The responses of the Cu and Au wires to repeated forward loading in torque control are shown in Fig. 3(a) and Fig. S2(c) in Ref. [27]. There is significant hysteresis with reverse plasticity occurring during unloading, which agrees with the results in twist control [Figs. 1(b) and 2] and with the predictions from the simulations [17,25,26]. Under the repeated load-unload sequences, plastic strain accumulates without monotonic hardening (also known as ratcheting deformation). A typical SEM image for the Cu wire after several cycles is given in Fig. 3(b). The slip traces indicated by the arrows show that local stress concentrations and a multiaxial stress state occur in certain regions.

Cyclic torsion data of Cu wires with different diameters are compared in Fig. 4. The shapes of the hysteresis loops for the three diameters are similar, but the magnitudes display a size effect. During the first forward loading, there is a systematic increase in monotonic hardening with decreasing diameter, while no size effect is found in uniaxial tension data [see Fig. S3(a) in Ref. [27]].

A quantitative comparison of our data with the literature is difficult, as conditions and protocols vary. Simulations do observe strong plastic recovery [17,25,26] but so far only in single-crystal wires below  $2 \mu\text{m}$  diameter. The simulations use much higher strain rates of  $4 \times 10^8 \text{ s}^{-1}$  for MD and  $8700 \text{ s}^{-1}$  for DDD. Comparing with other experiments, the load-unload method for torsion [2,28] does not observe the early plastic recovery. This is clearly an advantage of the torsion balance method here. On the other hand, both creep and the BE vary with time and with temperature [28]. Much more of the time-temperature space needs to be explored in future work.

We now consider the physical origin of the size effect and the recoverable plasticity observed. The size effect at initial yielding during the first forward loading [Fig. 4] is associated with the space available for the operation of dislocation sources, which in single-crystal specimens is the wire radius for torsion and the wire diameter for tension [2,29]. The grain size here is smaller than either of these length scales, and so we expect only a small size effect in any case but smaller in tension than torsion as observed [27]. Both theory and simulations show that torsional plasticity in single-crystal wires is obtained by the generation of geometrically necessary dislocations (GNDs) [1,2,4,17,25,26,30]. Under an applied torque, one dislocation of a dipole emitted from a source located inside of the specimen moves outward and may escape from the surface or be annihilated at grain boundaries. The

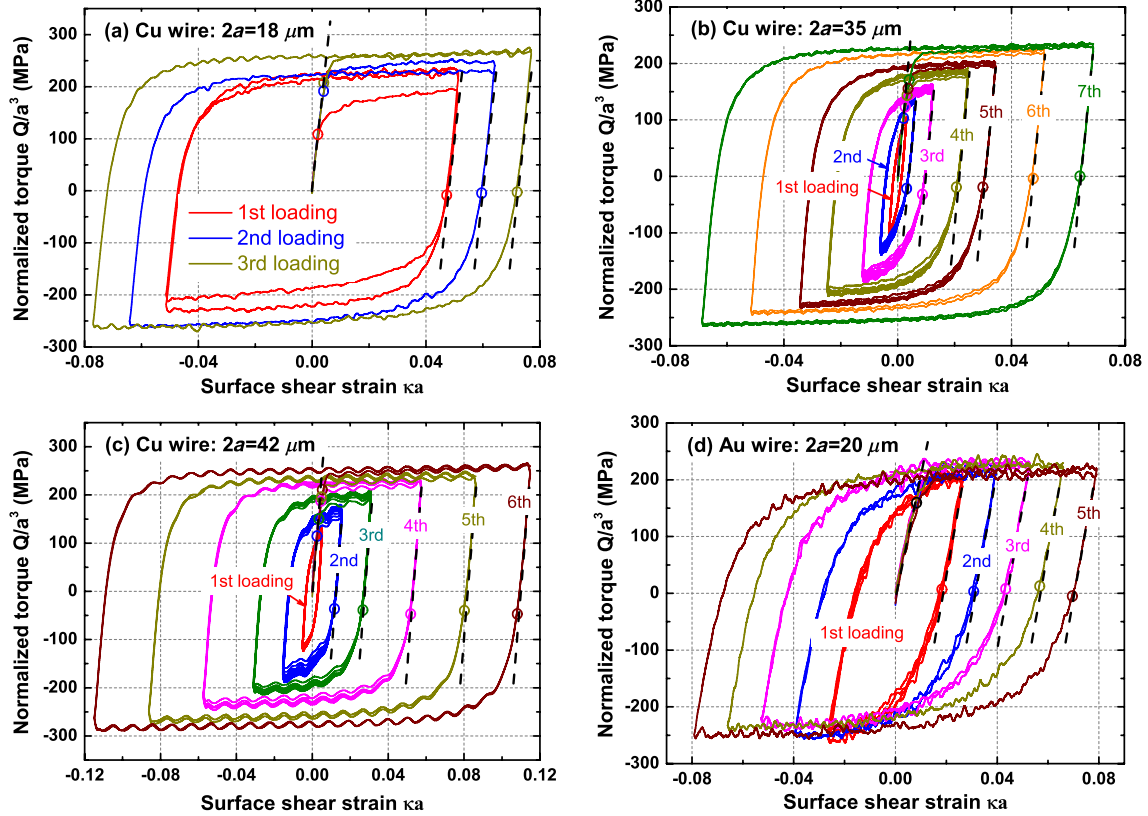


FIG. 2 (color online). Multiple cyclic responses of Cu and Au wires with increasing strain amplitudes in twist control: (a) Cu,  $2a = 18 \mu\text{m}$ , (b) Cu,  $2a = 35 \mu\text{m}$ , (c) Cu,  $2a = 42 \mu\text{m}$ , and (d) Au,  $2a = 20 \mu\text{m}$ . The elastic response is indicated by the dashed line, and the yield points in the forward and reverse directions are marked by circles. Oscillations in the curves are attributed to slight vertical misalignment.

other dislocation of the dipole moves towards the wire center under the stress gradient. These polarized dislocations cannot escape from the surface or move across the wire center due to the reversal of the sign of the stress at the neutral axis. As a result, axial GNDs with a screw component accumulate around the wire center during twisting. This process has been predicted theoretically [2,4,31] and confirmed by MD and DDD simulations [17,25,26]. A similar phenomenon in film bending has also been seen in DDD simulations [29,32]. On unloading or stress reversal the mutual repulsion (back-stress) of these dislocations pushes them outwards—some may disappear out of the sample surface—and so the specimen untwists; the BE and recoverable plasticity are observed here.

These ideas can be expressed more quantitatively. The amount of plastic twist  $\kappa_1$  due to a single axial screw dislocation is easily estimated—it is the Eshelby twist [33,34]. The shear strain due to the axial dislocation is  $\gamma_d = -b/(2\pi r)$  for  $r \in [r_0, a]$ , where a core cutoff radius  $r_0$  is introduced to avoid divergence in calculations. The elastic shear strain from the torsion is  $\gamma_r = \kappa r$  for  $r \in [0, a]$ . By adding the two strains and integrating the resulting elastic strain energy over the wire,

$$\begin{aligned}
 U &= \frac{1}{2} G \int_{r=0}^a 2\pi r (\gamma_d + \gamma_r)^2 dr \\
 &= \frac{1}{4} G \left[ \kappa a^2 (\pi \kappa a^2 - 2b) + 2\kappa b r_0^2 + \frac{b^2 \ln(a/r_0)}{\pi} \right]. \quad (1)
 \end{aligned}$$

Here, the dislocation core energy is neglected. Solving for the value of  $\kappa$  at which  $U$  is minimum, we obtain

$$\kappa_1 = \frac{b(a^2 - r_0^2)}{\pi a^4}. \quad (2)$$

Note that this is different from the standard expression for the Eshelby twist, which is as good a model for a single dislocation as the hollow core, and is more useful for estimating the Eshelby twist due to off-axis dislocations as done below. For  $r_0 \ll a$ , this corresponds to  $\kappa_1 a \sim 5\text{--}12$  microstrain for 50 and 20  $\mu\text{m}$  wires, respectively. This solution can be generalized to  $N$  dislocations close to the axis. In a continuum approximation (an infinite number of dislocations with infinitesimal Burgers vector), it can also be used for a ring of  $N$  dislocations parallel to the axis at a radius  $R$ . Within such a ring,  $\gamma_d$  vanishes, so we use  $\kappa_{NR} = N\kappa_1$  with  $r_0$  set to  $R$ .

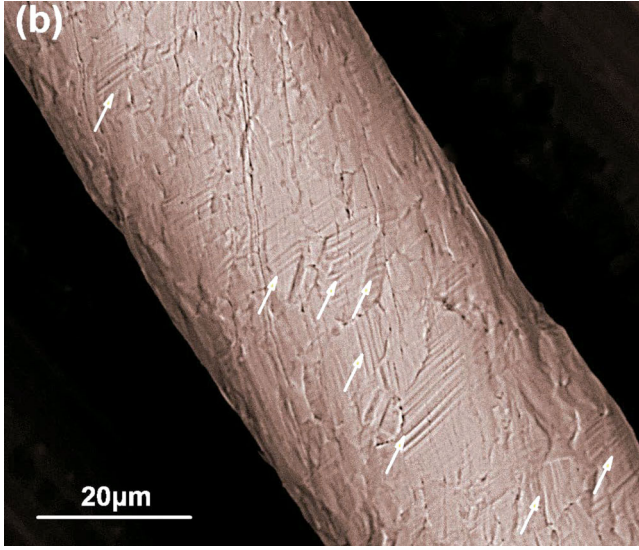
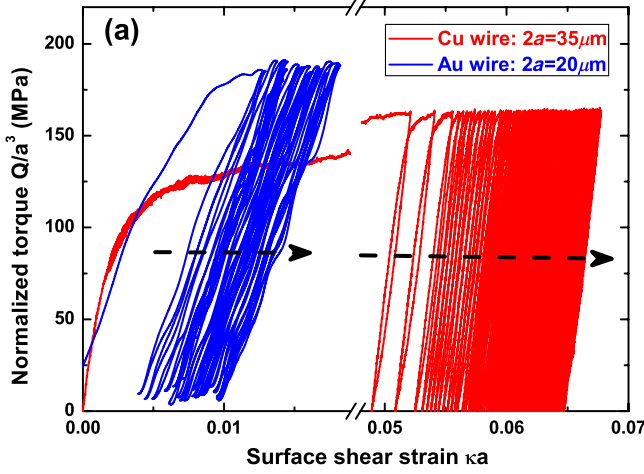


FIG. 3 (color online). (a) Responses of the Cu and Au wires to repeated forward loading. All load-unload cycles of both metals show a pronounced hysteresis. (b) SEM image of a Cu wire with  $2a = 42 \mu\text{m}$  after the test. The arrows point out distinct slip bands created by multiple slip systems.

In the DDD simulations to large twists, the dislocations are concentrated near the axis [17]. On unloading, the DDD shows that the bulk of the dislocations disappear from the wire, and hence complete plastic recovery may be expected except for the fraction of dislocations that become pinned or tangled [17]. In our polycrystalline wires, the dislocation motion is constrained by the grain boundaries. They will therefore be distributed throughout the cross section rather than concentrated near the axis. Upon unloading, they will be able to move outwards some fraction of the grain size  $d$ . Using Eq. (2) with  $r_0 = R$ , and with  $N$  dislocations, we have  $d\kappa_{NR}/dR = -2NbR/\pi a^4$ . Assuming a uniform distribution of  $N$  dislocations, the averages of  $\kappa_{NR}$  and its differential over  $0 < R < a$  (weighted by  $2\pi R$ ) are

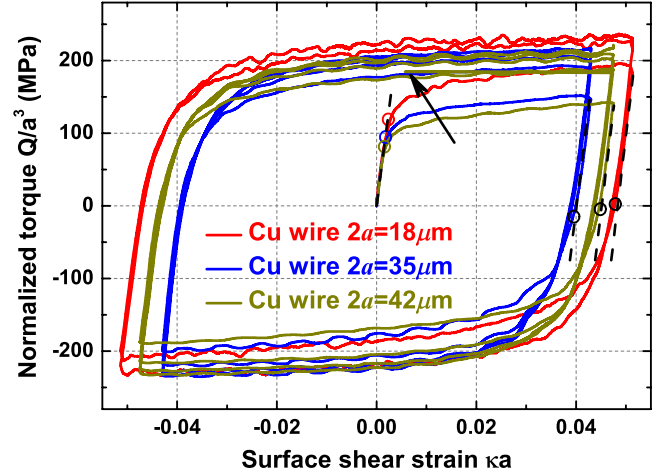


FIG. 4 (color online). Cyclic torsion data of the Cu wires with  $2a = 18, 35,$  and  $42 \mu\text{m}$  for the initial loading cycles. The yield points in the forward and reverse directions are marked by circles. The wires show significant Bauschinger and size effects.

$$\begin{aligned} \langle \kappa_{NR} \rangle &= \frac{1}{\pi a^2} \int_{R=0}^a 2\pi R \kappa_{NR} dR = \frac{Nb}{2\pi a^2}, \\ \langle d\kappa_{NR} \rangle &= -\frac{4Nb}{3\pi a^3} dR = -\frac{8}{3a} \langle \kappa_{NR} \rangle dR. \end{aligned} \quad (3)$$

Only a fraction of the dislocations can move. Many will be embedded in grain boundaries or otherwise pinned. Only a fraction will be axial; it is not clear if, e.g., radial dislocations will move so as to give plastic recovery. Those that can move within grains will on average move a distance  $\Delta R$ , which is only a fraction of  $d$ . The grain size here is only a fraction of the wire radius. So the plastic recovery  $\langle \Delta \kappa_{NR} \rangle$  is expected to be only a small fraction of the plastic torsion, in accordance with the recoveries seen in experiments.

In this picture, the BE is just that part of the plastic recovery which requires some reverse stress. The outward motion of the GNDs reduces the requirement to activate new dislocation sources for reverse plasticity. The higher hardening rate in the reverse response may then be attributed to the presence of higher densities of dislocations among slip systems. The creation of slip bands in Fig. 3(b) is primarily due to the increasing Peierls-Nabarro stress on the curved slip planes under torsion deformation [35]. Hence, the multiple slip system activation associated with additional local forest hardening appears. Interestingly, little or no recoverable plasticity was found in cyclic uniaxial tests [11,12,15]. This strongly implies that the GNDs induced by the inhomogeneous deformation are central to the BE and plastic recovery at small scales. Little cyclic hardening was observed in Au compared with Cu [Fig. 2]. One explanation is that gold has a lower stacking fault energy and less tendency for cross-slip, so that slip in Au is expected to be more planar [20].

In wire torsion, strong strain gradients appear, and hardening is due to the accumulation of both statistically stored dislocations and GNDs [1,4,17]. Some portion of plastic work is not dissipated but stored in the deformed materials through GNDs or other polarized structures [36]. This is the physical basis for the strain gradient plasticity (SGP) theories [18,37–39] with both energetic and dissipative length scales. It is beyond the scope of this Letter, but we will present elsewhere a nonlocal kinematic model within a SGP framework that captures the size effect, the BE, and plastic recovery.

This work was supported by the NSFC (Grants No. 11072084 and No. 11272131), the Specialized Research Fund for the Doctoral Program of Higher Education (Grant No. 20110142110039), and the Fundamental Research Funds for the Central Universities, HUST: Grants No. CXY12Q041 and No. 2011TS155. We thank the Analytical Testing Center of HUST for providing the SEM characterization.

\*Corresponding author.

ymhe@mail.hust.edu.cn

- [1] N. A. Fleck, G. M. Muller, M. F. Ashby, and J. W. Hutchinson, *Acta Metall. Mater.* **42**, 475 (1994).
- [2] D. J. Dunstan, B. Ehrler, R. Bossis, S. Joly, K. M. Y. P'ng, and A. J. Bushby, *Phys. Rev. Lett.* **103**, 155501 (2009).
- [3] D. Liu, Y. He, X. Tang, H. Ding, and P. Hu, *Scr. Mater.* **66**, 406 (2012).
- [4] D. Liu, Y. He, D. J. Dunstan, B. Zhang, Z. Gan, P. Hu, and H. Ding, *Int. J. Plast.* **41**, 30 (2013).
- [5] J. S. Stölken and A. G. Evans, *Acta Mater.* **46**, 5109 (1998).
- [6] J. R. Morris, H. Bei, G. M. Pharr, and E. P. George, *Phys. Rev. Lett.* **106**, 165502 (2011).
- [7] M. D. Uchic, D. M. Dimiduk, J. N. Florando, and W. D. Nix, *Science* **305**, 986 (2004).
- [8] S. Brinckmann, J.-Y. Kim, and J. R. Greer, *Phys. Rev. Lett.* **100**, 155502 (2008).
- [9] A. T. Jennings, M. J. Burek, and J. R. Greer, *Phys. Rev. Lett.* **104**, 135503 (2010).
- [10] J. Greer and W. Nix, *Phys. Rev. B* **73**, 245410 (2006).
- [11] D. C. Jang and J. R. Greer, *Nat. Mater.* **9**, 215 (2010).
- [12] Y. Xiang and J. J. Vlassak, *Acta Mater.* **54**, 5449 (2006).
- [13] L. Nicola, Y. Xiang, J. J. Vlassak, E. Van der Giessen, and A. Needleman, *J. Mech. Phys. Solids* **54**, 2089 (2006).
- [14] E. Demir and D. Raabe, *Acta Mater.* **58**, 6055 (2010).
- [15] D. Kiener, W. Grosinger, and G. Dehm, *Scr. Mater.* **60**, 148 (2009).
- [16] D. Kiener, C. Motz, W. Grosinger, D. Weygand, and R. Pippan, *Scr. Mater.* **63**, 500 (2010).
- [17] J. Senger, D. Weygand, O. Kraft, and P. Gumbsch, *Model. Simul. Mater. Sci. Eng.* **19**, 074004 (2011).
- [18] C. F. Niordson and B. N. Legarh, *J. Mech. Phys. Solids* **58**, 542 (2010).
- [19] J. Rajagopalan, J. H. Han, and M. T. A. Saif, *Science* **315**, 1831 (2007).
- [20] H. Zheng, J. Wang, J. Y. Huang, A. Cao, and S. X. Mao, *Phys. Rev. Lett.* **109**, 225501 (2012).
- [21] X. Y. Li, Y. J. Wei, W. Yang, and H. J. Gao, *Proc. Natl. Acad. Sci. U.S.A.* **106**, 16 108 (2009).
- [22] M. Koslowski, *Phys. Rev. B* **82**, 054110 (2010).
- [23] S. S. Shishvan, L. Nicola, and E. Van der Giessen, *J. Appl. Phys.* **107**, 093529 (2010).
- [24] S. Suresh, *Fatigue of Materials* (Cambridge University Press, Cambridge, England, 1998).
- [25] C. R. Weinberger and W. Cai, *J. Mech. Phys. Solids* **58**, 1011 (2010).
- [26] C. R. Weinberger and W. Cai, *Nano Lett.* **10**, 139 (2010).
- [27] See Supplemental Material at <http://link.aps.org/supplemental/10.1103/PhysRevLett.110.244301> for more details of the specimens, the extra experimental results, and a supporting discussion on the results.
- [28] A. J. Bushby, J. Feuvrier, D. V. Dong, and D. J. Dunstan, *Mater. Res. Soc. Symp. Proc.* **1424**, 61 (2012).
- [29] C. Motz and D. J. Dunstan, *Acta Mater.* **60**, 1603 (2012).
- [30] M. F. Ashby, *Philos. Mag.* **21**, 399 (1970).
- [31] J. Weertman, *Acta Mater.* **50**, 673 (2002).
- [32] C. Motz, D. Weygand, J. Senger, and P. Gumbsch, *Acta Mater.* **56**, 1942 (2008).
- [33] J. D. Eshelby, *J. Appl. Phys.* **24**, 176 (1953).
- [34] E. Akatyeva and T. Dumitrică, *Phys. Rev. Lett.* **109**, 035501 (2012).
- [35] B. Joós and M. S. Duesbery, *Phys. Rev. Lett.* **78**, 266 (1997).
- [36] A. A. Benzerga, Y. Bréchet, A. Needleman, and E. Van der Giessen, *Acta Mater.* **53**, 4765 (2005).
- [37] P. Gudmundson, *J. Mech. Phys. Solids* **52**, 1379 (2004).
- [38] M. E. Gurtin and L. Anand, *J. Mech. Phys. Solids* **53**, 1624 (2005).
- [39] L. Qiao, J. J. Rimoli, Y. Chen, C. A. Schuh, and R. Radovitzky, *Phys. Rev. Lett.* **106**, 085504 (2011).